Modulation of brainstem-cortical pathways by injection laryngoplasty in unilateral vocal fold paralysis: A Longitudinal diffusion MRI Case Study

Marie Dedry[A,B], Nicolas Delinte[B,C], Quentin Dessain[B,C], Arnaud Szmalec[A,B,D], Youri Maryn[E,F,G,H], Laurence Dricot[B] & Gauthier Desuter[I].

[A]Psychological Sciences Research Institute, Université catholique de Louvain, Louvain la-Neuve, Belgium
[B]Institute of Neuroscience, Université catholique de Louvain, Brussels, Belgium
[C]Institute of Information and Communication Technologies, Electronics and Applied Mathematics (ICTM), Université catholique de Louvain, Louvain-la-Neuve, Belgium
[D]Department of Experimental Psychology, Faculty of Psychology and Educational Science, University of Ghent, Ghent, Belgium
[E]European Institute for ORL-HNS, Department of Otorhinolaryngology and Head & Neck Surgery, ZAS Augustinus, Wilrijk, Belgium
[F]Department of Rehabilitation Sciences, Faculty of Medicine and Health Sciences, Ghent University, Ghent, Belgium
[G]Department of Speech-Language Therapy and Audiology, University College Ghent, Ghent, Belgium
[H]Phonanium, Lokeren, Belgium
[I]ENT , Head & Neck Surgery Department, University Hospital Antwerp (UZA), Edegem, Belgium

Corresponding author

Marie Dedry
Psychological Sciences Research Institute - IPSY
Place Cardinal Mercier 10/L3.05.01, 1348 Louvain-la-Neuve, Belgium
marie.dedry@uclouvain.be
0032 (0)472930622

Authors email address:

Marie Dedry: marie.dedry@uclouvain.be
Nicolas Delinte: nicolas.delinte@uclouvain.be
Quentin Dessain: quentin.dessain@uclouvain.be
Arnaud Szmalec: arnaud.szmalec@uclouvain.be
Youri Maryn: youri.maryn@gza.be
Laurence Dricot: laurence.dricot@uclouvain.be
Gauthier Desuter: gauthier.desuter@uza.be

ABSTRACT

Objective

This study investigates the potential role of injection laryngoplasty with hyaluronic acid in supporting spontaneous reinnervation and the recovery of vocal fold mobility, following unilateral vocal fold paralysis. Building on previous findings suggesting functional activation of the brainstem during a sustained vowel task before vocal fold mobility recovery (Dedry, Dricot, Van Parys, Boucquey, Delinte, van Lith-Bijl, Szmalec Maryn & Desuter, 2022), this study aims to explore the neural plasticity in response to this peripheral intervention. Specifically, we hypothesize that this intervention may not only activate brainstem regions of interest but also induce changes in the motor and sensory pathways associated with phonation.

Methods

A longitudinal single-case study was conducted on a 54-year-old woman (P3) with right-sided unilateral vocal fold paralysis. P3 received a hyaluronic acid injection laryngoplasty into the paralyzed vocal fold, along with a sham behavioral voice therapy. Assessment sessions, including MRI scans (structural, functional, and diffusion), were conducted at four time points to examine potential neural changes. Diffusion MRI and tractography were used to assess microstructural changes in brainstem-to-cortex motor and sensory pathways. The same assessment protocol was followed by a matched healthy control participant for comparison. Diffusion data were preprocessed and modeled using the DIAMOND model, focusing on the corticobulbar and medial lemniscal tracts.

Results

A marked increase in weighted fractional anisotropy was observed in left and right anterior motor tracts of interest between the first and second sessions, shortly after

the hyaluronic acid injection. These values remained stable thereafter. In contrast, the posterior sensory tracts showed minimal change over time, with weighted fractional anisotropy values remaining lower than those of the control participant.

Conclusion

Although limited to a single case, the bilateral improvements observed in motor tract integrity, reflected by increased fractional anisotropy shortly after the hyaluronic acid injection, suggest a possible neuroplastic response, particularly within the corticobulbar projections. These findings indicate that early injection laryngoplasty may promote adaptive structural changes in motor pathways involved in phonation, potentially supporting reinnervation following unilateral vocal fold paralysis.

KEYWORDS

Unilateral vocal fold paralysis, injection laryngoplasty, diffusion MRI, brain plasticity, nerve recovery, voice recovery.

1. Introduction

The present case study adopts an exploratory approach to investigate whether and how the injection laryngoplasty using hyaluronic acid into a paralyzed vocal fold could, in certain cases, support the process of spontaneous reinnervation and recovery of vocal fold mobility. Findings from our previous study [1] suggested that, in the only patient who received the injection augmentation, functional magnetic resonance imaging (MRI) indicated bilateral activation in brainstem regions corresponding to the motor and sensory nuclei during a sustained vowel phonation task. At the time of this activation, the patient had not yet regained mobility of the vocal fold, as assessed by videostroboscopy, and the results of the laryngeal electromyography were consistent with vocal fold paralysis. There was no clinical indication at that point that spontaneous reinnervation was likely to occur. This observation raises the possibility that a peripheral intervention—namely, the injection of a biologically inert substance solely intended to medialize the vocal fold—could elicit a response in the central nervous system at the level of the brainstem. Approximately three months after the injection, the patient retrospectively identified a perceptible shift during which her voice progressively regained its normal quality. By the time of full recovery, the patient had regained complete vocal fold mobility along with a functionally satisfactory voice. To further substantiate the hypothesis of potential central neural responses to this peripheral procedure, the present study focuses on diffusion MRI sequences acquired concurrently for the same patient.

To provide anatomical context for interpreting these diffusion MRI findings, the following sections describe the motor and sensory pathways associated with phonation. The corticobulbar tract is the primary pathway involved in motor control of the laryngeal musculature, and consequently, the vocal folds [2]. It originates in the

laryngeal motor cortex, travels through the corona radiata, and then passes through the internal capsule [3]. Although it is traditionally accepted that this tract passes through the genu of the internal capsule [4], some authors have reported that these fibers may instead course more posteriorly, through regions extending beyond the midway point of the posterior limb of the internal capsule [3]. Pan et al. [5] provided further details and described a somatotopic organization of corticobulbar fibers within the internal capsule. They proposed an anteroposterior alignment of these fibers along the long axis of the posterior limb, with fibers innervating the laryngeal and tongue muscles occupying the most anterior position. After the internal capsule, the fibers continue through the crus cerebri of the midbrain, then through the anterior portion of the pons and medulla oblongata, where they ultimately synapse with the motor fibers of the vagus nerve at the level of the nucleus ambiguus (located in the ventral part of the medulla) [6]. Furthermore, the right and left corticobulbar tracts have been described as exhibiting a generally symmetrical anatomical organization [5,7,8]. It is important to acknowledge that, although it is widely accepted that these tracts predominantly decussate, with a minority of fibers remaining ipsilateral [9], the precise anatomical location of this decussation is rarely described in neuroanatomical textbooks and remains unclear. Research on the localization of the corticobulbar tract to the facial nucleus has suggested that corticobulbar tract decussation may occur at the level of the ambiguus nuclei [10,11]. However, because these nuclei span a considerable longitudinal distance, it is not possible to accurately pinpoint the exact site of decussation. It is also possible that the decussation does not occur at a single, distinct site, but rather over a broader area, with fibers crossing at different points.

Sensory information reaching the solitary tract nuclei via the internal branch of the superior laryngeal nerve and the posterior branch of the recurrent laryngeal nerve is

relayed through a pathway involving direct connections between the solitary tract nuclei and the ambiguus nuclei [12]. These connections are mediated by interneurons located in the brainstem's reticular formation, which is crucial for integrating and modulating sensory input [13]. These presumed polysynaptic relays, supported by clinical evidence from studies of laryngeal reflexes, facilitate the integration of sensory and motor pathways, thereby enabling coordinated control of sensory inputs and motor responses [13].

To our knowledge, no published studies have reported diffusion imaging findings in patients with vocal fold paralysis. However, several studies have identified microstructural alterations in the corticobulbar tract in disorders involving phonation or related functions, such as articulation or swallowing. These include conditions such as dysarthria [e.g.,14], apraxia of speech [e.g.,2], dysphagia [e.g.,15], hypophonia due to subcortical vascular cognitive impairment [e.g., 16], and laryngeal dystonia [e.g., 4]. Although these studies involve partially overlapping neural regions, the origin of the impairment in all these cases was central nervous system damage, rather than peripheral nerve injury, as seen in cases of unilateral vocal fold paralysis (UVFP). One of these studies specifically examined the effects of an intervention. The study by Fiori et al. [2] demonstrated an improvement in the microstructure of the corticobulbar tracts following a multimodal speech motor treatment in children with apraxia of speech. They compared the data from five children who received targeted speech motor intervention (PROMPT treatment) with those from five other children with the same disorder who underwent non-speech oral motor exercises. The authors reported an increase in fractional anisotropy and a reduction in mean diffusivity in the left dorsal corticobulbar tract, corresponding to the representation of the lips in the homunculus, specifically for the PROMPT group. Additionally, they observed

increased fractional diffusivity with no change in mean diffusivity in the left ventral corticobulbar tract, corresponding to the representation of the tongue and larynx, for both intervention groups. The hand corticospinal tract was used as a control and showed no differences. It is important to note that the intervention consisted of 50 sessions, each lasting 45 minutes, with an approximate frequency of two sessions per week. This study suggests that diffusion MRI can reveal treatment-induced structural brain plasticity, although spontaneous and progressive maturation over a period of 6 months during childhood was not controlled.

The aim of the present study is to further investigate the neural plasticity that may occur following an injection augmentation in the paralyzed vocal fold due to peripheral laryngeal recurrent nerve injury. Indeed, if this injection leads to functional activation of brainstem regions corresponding to the motor and sensory nuclei [1], we hypothesize that cerebral plasticity extends beyond this level, also inducing changes in the motor and sensory pathways involved in phonation.

2. Methods

The present study builds on the findings of Dedry et al. [1], which details the experimental design. It specifically focuses on the diffusion MRI sequences, acquired concurrently with the previously reported fMRI data.

2.1 Participants

The protocol of this longitudinal case study was approved by the Ethics Committee of the University Hospital of Saint-Luc (number: B403201837695) and was carried out with respect to the standards of the Declaration of Helsinki. The inclusion criterium for the study was to have had a UVFP for less than 3 months.

The third patient of the study of Dedry et al. [1] (P3) is a 54-year-old right-handed woman diagnosed with a right-sided UVFP in the abductory position. She reported the onset of symptoms 41 days prior to inclusion in the study, following an upper

respiratory tract infection. The control participant (C) was a 55-year-old right-handed woman. A healthy control was selected to provide a reference for normal phonation and somatosensory feedback, which was central to the study's hypothesis. Both women were native French speakers.

2.2 Intervention and assessment procedures

P3 was treated with a hyaluronic acid injection (1 ml) administered via a suprathyroidal approach into the right, paralyzed vocal fold. The procedure was performed under local anesthesia under laryngoscopic guidance. She also underwent a placebo behavioral voice therapy consisting of exercises specifically intended to avoid active mobilization of the vocal folds. The program aimed to reduce maladaptive compensatory behaviors, facilitate relaxation of the neck and shoulder muscles, and improve breathing efficiency and alignment. Previous work [17] has shown that similar sham protocols have minimal impact on objective voice measures in participants without dysphonia, and in the case of P3, exercises without active vocal fold mobilization would not be expected to enable glottic closure. The healthy control participant did not undergo any therapeutic procedure or sham intervention.

Assuming the presumed date of nerve injury as day 0, P3 participated in four assessment sessions on days 41 (T1), 83 (T2), 218 (T3), and 315 (T4), with a hyaluronic acid injection administered on day 60. A multiparametric evaluation was carried out at each of these four time points, which has been thoroughly described in Dedry et al. [1]. At the time of study inclusion, P3's hearing was assessed and found to be normal. UVFP was confirmed through videostroboscopy. Laryngeal electromyography (LEMG) was performed on the right and left thyroarytenoid and cricothyroid muscles using concentric needle electrodes (recording area: 0.07 mm^2; length: 37 mm; diameter: 0.46 mm), connected to a Nicolet™ Viking AT2+6 amplifier system. Recordings of the thyroarytenoid muscles were taken at rest, during

sustained phonation of [a:] at habitual pitch and loudness (≥3 sec), and during three sniff inspirations. Cricothyroid muscle activity was recorded during high-pitched [i:] phonation. EMG data were qualitatively interpreted by a multidisciplinary team, and volitional activity in the paralyzed-side thyroarytenoid muscle during phonation was rated on a 4-point scale. LEMG results revealed damage localized to the lower part of the vagus nerve pathway, with preservation of the superior laryngeal nerve as the signal observed in the cricothyroid muscle was normal. Scale-coding of qualitative LEMG for the right thyroarytenoid muscle showed a score of 4: “single fiber activity” at times T1 and T2, and 1: “dense volitional activity” at times T3 and T4 [18].

2.3 Neuroimaging assessment

P3 also underwent four MRI scans at the previously mentioned time points, which included anatomical, functional (resting-state and task-based), and multi-shell diffusion sequences. The control participant underwent the same MRI protocol, with day 0 serving as the first assessment and the same inter-session intervals maintained throughout the study.

2.3.1 Imaging acquisition parameters and data pre-processing

MRI sequences were obtained at the Cliniques Universitaires Saint-Luc (UCLouvain, Belgium) on a 3T GE SIGNA^{TM} Premier scanner (GE Healthcare, Chicago, IL) fitted with a 48-channel coil. The diffusion MRI parameters were as follows: repetition time (TR) = 4837 ms, echo time (TE) = 80 ms, in-plane field of view (FOV): 220 × 220 mm², matrix size: 110 × 110, 68 slices, slice thickness = 2 mm, 2 mm isotropic voxels, Δ = 35.7 ms, δ = 22.9 ms, 168 directions with 64 gradients at b = 1000, and 32 gradients at b = 2000, 3000, and 5000 s/mm², corresponding to diffusion gradient intensities up to 68.9 mT/m, with 7 interspersed b0 images.

A three-dimensional (3D) T1-weighted data set encompassing the whole brain was acquired to provide detailed anatomy (1 mm³) with a MPRAGE sequence

(inversion time = 900 msec, TR = 2188.16 ms, TE = 2.96 ms, flip angle = 8°, FOV = 256 × 256 mm², matrix size = 256 × 256, 156 slices, slice thickness = 1 mm, 1mm isotropic voxels, no gap).

The preprocessing of the diffusion data was carried out using the Elikopy pipeline [19], which involved brain extraction [20], thermal denoising [21], as well as correction for Eddy-current distortions and head motion [22]. Noise and motion during the scan were estimated using QUAD [23].

2.3.2 Microstructural model

The DIAMOND model [24] was selected to assess microstructural differences across the four time points. DIAMOND is a multi-fixel model, which allows to represent the diffusion signal as the sum of multiple *fixels*, i.e., fiber populations per voxel. It provided tensor-derived metrics, including fractional anisotropy (FA), axial diffusivity (AD), radial diffusivity (RD), and mean diffusivity (MD) for each estimated fixel, as well as an estimated volume fraction. FA measures the direction of water diffusion, with higher values indicating intact, well-organized white matter while lower values suggest potential damage to neural fibers. AD reflects the diffusion of water molecules along the primary direction of the fibers, while RD quantifies diffusion perpendicular to this main axis. MD represents the average diffusivity for a given fixel.

Each voxel was modeled with two fiber populations and an isotropic signal, with a volume fraction assigned to each compartment. The diffusivity of the isotropic compartment was set at 3×10^{-9} m²/s to correspond to the diffusion coefficient of free water at 37°C [25].

2.3.3 Tracking of the tracts of interest (TOIs)

Streamlines traversing the nucleus ambiguus (NA) and the solitary tract nucleus (SN) were reconstructed from diffusion-weighted imaging data to define two

tracts of interest (TOIs) in each hemisphere: an anterior tract passing through the motor-associated nucleus ambiguus in the anterior medulla oblongata, and a posterior tract passing through the sensory-associated solitary tract nucleus in the posterior medulla oblongata. Local fiber orientation distributions were estimated via the multi-shell, multi-tissue constrained spherical deconvolution (MSMT-CSD) algorithm [26], and probabilistic tractography was performed using the iFOD2 algorithm [27], both implemented in the MRtrix3 toolbox (version 3.0.3; [28]). The seed regions were defined based on activations identified through functional MRI during a sustained phonation task described in Dedry et al. [1]. These activation sites were localized in the voice-related motor nucleus on the left and the sensory nucleus on the right within the medulla oblongata (Figure 1A) and were identified at the time point following the hyaluronic acid injection into P3's paralyzed vocal fold [1]. The fMRI activation clusters were thresholded and binarized to obtain binary regions of interest (ROIs). Given the lateralized distribution of the observed activation clusters, homologous regions in the contralateral hemisphere were obtained by applying a mid-sagittal symmetry transformation. Although these ROIs are broader than the size of the nuclei, they include the white matter fibers that emanate from them. The functional ROIs were registered using rigid transformations to each time point of the participant.

Additional ROIs were positioned in the superior part of the pons to constrain the analysis to tracts originating from the NA and SN, thereby minimizing interference from parallel fiber pathways located superior to the pons. The ROIs were drawn in Montreal Neurological Institute (MNI) space and registered to the native space of each scan of the participant using a Python implementation of the ANTS algorithm

[29], which employed rigid and affine transformations to optimize the mutual information between each time point.

More specifically, the tractography parameters were:

- **For the streamlines passing through the NA:** 1 500 000 seeds were placed in the NA ROI with two inclusion ROIs in the pyramids represented in orange in Figure 1C.
- **For the streamlines passing through the SN:** 10 000 seeds were placed in the SN ROI with an inclusion ROI in the medial lemniscus displayed in cyan in Figures 1B and 1C.

In both cases, the maximum angle between tractography steps was set to 15° and the streamlines were generated from the seed point in one direction only. The number of seeds was limited instead of the number of streamlines to avoid reaching a hard threshold in the streamline number. Tractography was performed in P3's native space.

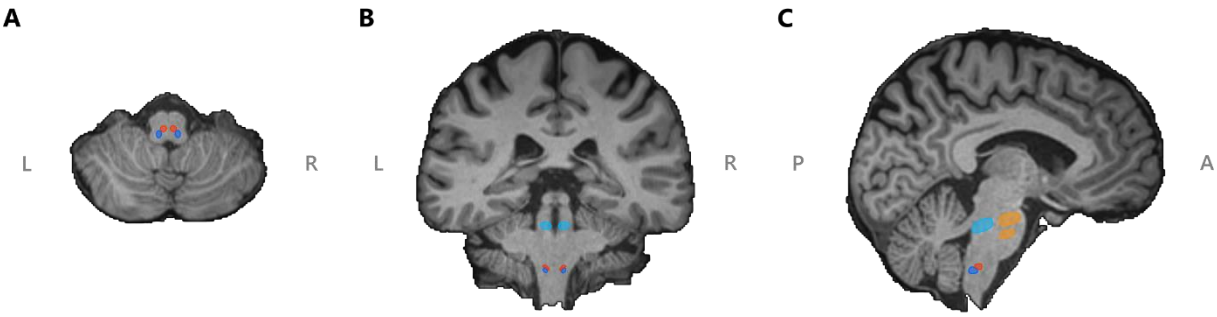

Figure 1: Placeholder.
Notes. **A:** Axial view of the activation clusters for the NA (in red) and SN (in blue), obtained from functional MRI on P3. **B & C:** Coronal and sagittal views of the activation clusters (in red and blue), along with the additional inclusion ROIs in the pyramids (in orange) and medial lemniscus (in cyan), all presented in P3's native space.

2.3.4 Tract microstructure analysis

The microstructural model produced tensor-derived metrics for each fixel. To obtain a single representative value per tract, the metric maps were combined into a single aggregated map by weighting each fixel's contribution according to its

estimated fiber volume fraction. Thereby attributing a higher contribution to the dominant fiber population and yielding volume-weighted metrics (wFA, wAD, wRD, wMD), as described by Delinte et al. [30]. Mean metric values for each tract were then calculated by averaging the metric values within the corresponding tract-based ROIs.

Since no nuclei activation was observed in the control participant, the streamlines found in P3 were spatially normalized to MNI space to facilitate the analysis of equivalent regions. Binary ROIs were generated by selecting voxels traversed by the streamlines and then projected into the native space of the control participant.

The metric values and standard deviations from the control participant were used as a reference to qualitatively assess individual changes in P3 by interpreting Z-scores. This was applied because of the absence of activation in the nuclei of interest in the control participant and the limitation of having only one control subject, which prevented the use of other analytical methods.

3. Results

3.1 Tract of interest

Attempts to identify decussating fibers were inconclusive, as tractography predominantly revealed ipsilateral projections. These tracts are illustrated in P3's native space in Figure 2. The absence of contralateral fibers further supports the interpretation that the TOIs are located rostral to the decussation sites of both the corticobulbar tract and the medial lemniscal tract.

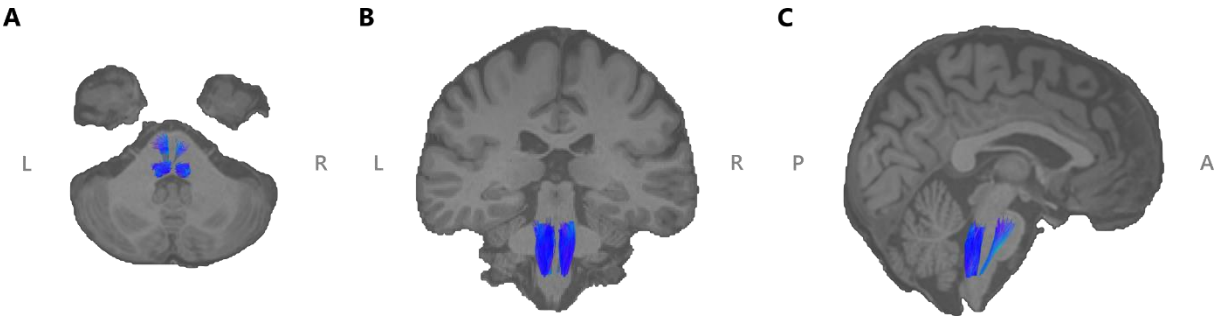

Figure 2: Tract of interest in P3.
Notes. Axial (**A**), coronal (**B**), and sagittal (**C**) views presented in P3's native space.

3.2 Qualitative analysis of weighted FA values

Table 1 provides the weighted FA (wFA) values for the two (anterior and posterior) bilateral TOIs across the four time points for P3. Additionally, it presents the overall mean wFA value and standard deviation (SD) for the control participant (C), averaged across the four time points, computed within the same tracts traced in P3 and projected into the control participant's native space. The lower table section reports the corresponding standard scores (Z scores).

Table 1. Weighted FA (wFA) values for the two bilateral tracts of interest (TOI) across the four time points.

	Right **Anterior** TOI	Left **Anterior** TOI	Right **Posterior** TOI	Left **Posterior** TOI
wFA **P3T1**	0.654	0.694	0.666	0.589
wFA **P3T2**	0.740	0.745	0.637	0.628
wFA **P3T3**	0.734	0.759	0.656	0.615
wFA **P3T4**	0.732	0.752	0.655	0.594
Mean **wFA** C	0.745	0.801	0.710	0.695
SD **wFA** C	0.017	0.006	0.010	0.013
Z-score **T1**	-5,28	-18,17	-4,27	-8,18
Z-score **T2**	-0,30	-9,44	-7,08	-5,13
Z-score **T3**	-0,63	-7,12	-5,25	-6,18
Z-score **T4**	-0,74	-8,21	-5,35	-7,79

Notes. P3 refers to patient 3, and C refers to the control participant. T indicates the timing of the assessment session (T1, T2, T3 or T4).

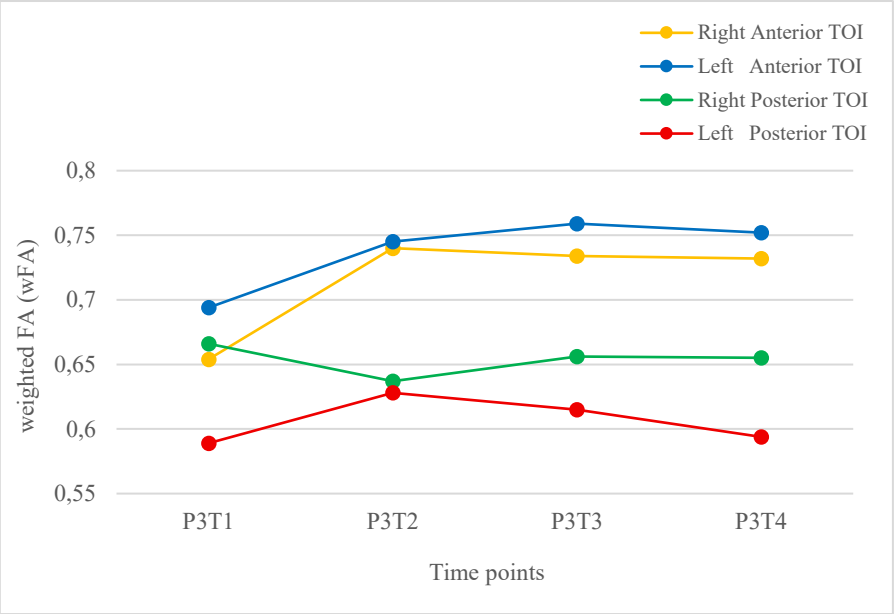

Figure 3: Weighted FA (wFA) values for the TOIs in P3.
Notes. P3 refers to patient 3, and C refers to the control participant. T indicates the timing of the assessment session (T1, T2, T3 or T4).

In the right and left anterior TOIs (motor), a noticeable improvement in wFA values is observed between T1 and T2. To reiterate, T2 refers to the assessment conducted following the injection of hyaluronic acid into the paralyzed right vocal fold of P3. After this second assessment, wFA values remain relatively stable over time. On the right side, corresponding primarily to the nerve fibers from the non-paralyzed left vocal fold, the z-score values normalize. On the left side, corresponding primarily to the nerve fibers from the paralyzed right vocal fold, the z-scores remain consistently deficient (Figure 3).

In the posterior TOIs (sensory), the results are less clear, with wFA values showing minimal variation over time. No important changes are observed after the hyaluronic acid injection (T2), nor during voice recovery (after T3). The values remain consistently lower at all assessment points compared to the control participant. The values on the left, corresponding to the nerve fibers from the paralyzed right vocal fold, are lower than those of the right posterior TOI (Figure 3).

4. Discussion

The results reveal an unexpected pattern of microstructural changes, with the most pronounced changes occurring in the anterior tracts reaching the region of the motor ambiguus nuclei. In the lower portion of the corticobulbar tracts, wFA values show a marked increase at T2, following the injection, in both the right and left tracts. Subsequently, at T3 and T4, the wFA values stabilize on both sides. Although wFA values in the right corticobulbar tract, which corresponds to the nerve fibers innervating the non-paralyzed left vocal fold, reached levels comparable to those of the control participant, the normalization of the Z-scores in this tract must be interpreted with caution due to the difference in wFA values observed in the control participant's tracts. In contrast, minimal variations are observed in the sensory medial lemniscal tracts, which originate from the more posterior region of the medulla in the brainstem, where the nuclei of the solitary tract are located.

Our initial hypothesis, supported by our previous study, was that restoring somatosensory feedback could induce neuromodulatory changes, potentially facilitating nerve recovery. Accordingly, we expected to observe primarily a sensory response [1]. However, as previously mentioned, it is within the motor tracts that variations were observed, at the time point following the injection. It has been reported that sensory information from the larynx can be directly transmitted from the solitary tract nuclei to the motor ambiguus nuclei within the reticular formation of the brainstem [13]. Since we cannot directly observe the transmission of information via this pathway within the brainstem, we can only hypothesize that their integration may contribute to the observed improvement in the structural integrity of the bilateral descending motor tracts. This bilateral improvement also supports that the nerves transmitting somatosensory information were preserved not only on the healthy left

side, but also partially the paralyzed side. Indeed, for our patient, the right superior laryngeal nerve was preserved, as confirmed by LEMG, and the right recurrent laryngeal nerve, which may play a role in the sensory innervation of the subglottic area, was affected due to an infectious etiology, suggesting that some sensory components may have remained functional. Fields [31] wrote a review on how changes in the activity level of a neural circuit and/or experience-dependent learning influence not only synaptic connections but also the structure and function of axons through myelination. He formulated several hypotheses on how glial cells along axons might detect changes in functional activity, and on how myelination could be improved, either by myelinating unmyelinated axons, changing the thickness of the myelin sheath, or modifying the structure or the interdistance of the nodes of Ranvier. The review also reported that these changes could occur within a very short time frame. It is therefore reasonable to hypothesize that the restoration of somatosensory feedback may change the activity level of the phonation circuit, thereby inducing bilateral modifications in the anatomical integrity of the tracts involved. These same processes could also contribute to supporting reinnervation of the recurrent laryngeal nerve [31].

We outline below the methodological limitations encountered, along with the rationale behind the decisions made to address them. First, it was difficult to find precise information regarding the decussation of the corticobulbar tracts in the literature and anatomical atlases. Available sources indicated that corticobulbar tract decussation occurs at the level of the ambiguus nuclei [10,11]. However, given the spatial resolution of the diffusion MRI sequences which required a trade-off with scan duration, our protocol did not allow for the inclusion of the caudal brainstem, and therefore not the full rostro-caudal extent of the ambiguus nuclei. We attempted to

identify both ipsilateral and crossed fibers through tractography, but the reconstruction of the decussating fibers was unsuccessful. Based on the reported location of the decussation and the absence of crossed fibers in our tractography results, we inferred that our analysis was performed above the level of decussation. Consequently, we assumed that measurements in the left tracts corresponded to the paralyzed right vocal fold, and values in the right tracts corresponded to the mobile left vocal fold. Second, tractography was the most suitable and feasible method for estimating the course of the corticobulbar tracts. To improve the accuracy of corticobulbar tractography and better capture the full extent of the brainstem, a multishell diffusion sequence focused specifically on the brainstem could be used. This would provide optimized spatial resolution for the relevant nuclei, but it would exclude the laryngeal motor cortex. The trade-offs of this targeted approach should therefore be carefully considered. Third, in the control participant, no activation was observed in the regions of the ambiguus or solitary tract nuclei during the sustained vowel phonation task in functional MRI. It was therefore not possible to reconstruct tracts from these regions in the control participant, as it was done for the patient. In order to estimate the extent of the changes observed in the patient, we projected the tracts obtained from P3 into the native space of the control participant. This approach enabled the extraction of the control's mean and standard deviation of wFA values, allowing the computation of a Z-score for qualitative comparison. While this methodological approach does not allow for strong inferential conclusions, it represents the most appropriate strategy given the nature and limitations of the available data. Ideally, patient data should be compared to a pool of control participants to ensure that the changes observed in the patient do not appear in any of the controls. In future studies, it would also be useful to diversify phonation tasks in

control participants to elicit sufficient activation in both motor and sensory nuclei of the voice. To enhance brainstem motor nuclei activation and improve fMRI localization, tasks such as glottal stops and sirens on sustained vowels could be incorporated, potentially engaging the laryngeal musculature more actively. This would ensure consistent tractography across patients and participants using the same parameters, while allowing for the quantification of subject-specific wFA values along the tracts. Fourth, the processes of plasticity that drive changes in fractional anisotropy values remain difficult to interpret. Further studies investigating the cellular mechanisms of white matter plasticity are needed to deepen our understanding of these processes [31]. Finally, this case study does not allow to distinguish recovery influenced by injection laryngoplasty from spontaneous recovery. Nevertheless, this does not diminish the relevance of our research hypotheses and findings regarding the potential neuromodulatory effects of injection laryngoplasty, which appear to extend beyond purely peripheral or mechanical mechanisms. Further studies involving multiple individual patients will be necessary to clarify the relative contributions of spontaneous recovery and injection-induced neural changes.

5. Conclusion

Although this is a single-case study, the results provide preliminary insights into the possibility that early injection laryngoplasty could lead to bilateral microstructural changes, reflected by increased fractional anisotropy, in corticobulbar tracts involved in the motor control of phonation. These findings highlight the potential role of restoring somatosensory feedback through early peripheral interventions, which may influence neuromodulatory responses and support spontaneous reinnervation following unilateral vocal fold paralysis. This study also raises questions about the location of the decussation of these motor tracts and offers suggestions for improving its identification.

References

1. Dedry M, Dricot L, Van Parys V, Boucquey D, Delinte N, van Lith-Bijl J, Maryn Y, Szmalec A, Desuter G. Brain adaptation following various unilateral vocal fold paralysis treatments: a magnetic resonance imaging based longitudinal case series, Front Neurosci. 2022;16:947390. https://doi.org/10.3389/fnins.2022.947390
2. Fiori S, Pannek K, Podda I, Cipriani, P, Lorenzoni V, Franchi B, Pasquariello R, Guzzetta A, Cioni G, Chilosi A. Neural changes induced by a speech motor treatment in childhood apraxia of speech: a case series. J Child Neurol. 2021;36(11):958-967. https://doi.org/10.1177/08830738211015800.
3. Yim SH, Kim JH, Han ZA, Jeon S, Cho JH, Kim GS, Choi S-A, Lee JH. Distribution of the corticobulbar tract in the internal capsule. J Neurol Sci. 2013;334(1-2):63-8. https://doi.org/10.1016/j.jns.2013.07.015
4. Simonyan K, Tovar-Moll F, Ostuni J, Hallett M, Kalasinsky VF, Lewin-Smith MR, Rushing EJ, Vortmeyer AO, Ludlow CL. Focal white matter changes in spasmodic dysphonia: a combined diffusion tensor imaging and neuropathological study. Brain. 2008;131(Pt 2):447-59. https://doi.org/10.1093/brain/awm303
5. Pan C, Peck KK, Young RJ, Holodny AI. Somatotopic organization of motor pathways in the internal capsule: a probabilistic diffusion tractography study. AJNR Am J Neuroradiol. 2012;33(7):1274-80. https://doi.org/10.3174/ajnr.A2952
6. Afifi AK, Bergman RA. Functional neuroanatomy: text and atlas (2nd ed). New-York, McGraw-hill; 2005.
7. Liégeois FJ, Butler J, Morgan AT, Clayden JD, Clark CA. Anatomy and lateralization of the human corticobulbar tracts: an fMRI-guided tractography

study. Brain Struct Funct. 2016;221(6):3337-45. https://doi.org/10.1007/s00429-015-1104-x

8. Simonyan K, Ostuni J, Ludlow CL, Horwitz B. Functional but not structural networks of the human laryngeal motor cortex show left hemispheric lateralization during syllable but not breathing production. J Neurosci. 2009;29(47):14912-23. https://doi.org/10.1523/JNEUROSCI.4897-09.2009
9. Jürgens U. Neural pathways underlying vocal control. Neurosci Biobehav Rev. 2002;26(2):235-58. https://doi.org/10.1016/s0149-7634(01)00068-9
10. Kanbayashi T, Sonoo M. The course of facial corticobulbar tract fibers in the dorsolateral medulla oblongata. BMC Neurol. 2021;21(1):214. https://doi.org/10.1186/s12883-021-02247-z
11. Kim YK, Kim YB, Suh BC, Jeong YH, Ann S, Chung PW. Topographic consideration on the occurrence of ipsilesional facial paresis in lateral medullary infarction. Cerebrovasc Dis. 2024;53(1):38-45. https://doi.org/10.1159/000530986
12. Foote AG, Thibeault SL. Sensory innervation of the larynx and the search for mucosal mechanoreceptors. J Speech Lang Hear Res. 2021;64(2):371-391. https://doi.org/10.1044/2020_JSLHR-20-00350
13. Sulica L, Carey B, Branski RC. A novel technique for clinical assessment of laryngeal nerve conduction: normal and abnormal results. Laryngoscope. 2013;123(9):2202-8. https://doi.org/10.1002/lary.23950
14. Liégeois F, Tournier JD, Pigdon L, Connelly A, Morgan AT. Corticobulbar tract changes as predictors of dysarthria in childhood brain injury. Neurology. 2013;80(10):926-32. https://doi.org/10.1212/WNL.0b013e3182840c6d

15. Im S, Han YJ, Kim S-H, Yoon M-J, Oh J, Kim Y. Role of bilateral corticobulbar tracts in dysphagia after middle cerebral artery stroke. Eur J Neurol. 2020;27(11):2158-2167. https://doi.org/10.1111/ene.14387
16. Yoon JH, Ahn Y, Kim SH, Chin J, Park S, Na DL. Neuroanatomical correlates of hypophonia in subcortical vascular cognitive impairment. Eur Neurol. 2017;78(1-2):93-104. https://doi.org/10.1159/000479023
17. Maryn Y, Dedry M, de Mahieu V, Fournier-Foch J. Toward sham interventions for behavioral voice treatment outcome research in female students without dysphonia. J Voice. 2024;S0892-1997(24)00271-6. https://doi.org/10.1016/j.jvoice.2024.08.023
18. Kneisz L., Volk GF, Mayr W, Leonhard M, Pototschnig C, Schneider-Stickler B. Objectivation of laryngeal electromyography (LEMG) data: turn number vs. qualitative analysis. Eur Arch Otorhinolaryngol. 2020;277(5):1409-1415. https://doi.org/10.1007/s00405-020-05846-7
19. Dessain Q, Simon M, Delinte N. Hyedryn/elikopy [computer software]. v0.4. Zenodo; 2024. https://doi.org/10.5281/zenodo.10514465.
20. Otsu N. A threshold selection method from gray-level histograms. Automatica. 1975;11(285-296):23-27. https://doi.org/10.1109/TSMC.1979.4310076
21. Veraart J, Novikov DS, Christiaens D, Ades-Aron B, Sijbers J, Fieremans E. Denoising of diffusion MRI using random matrix theory. Neuroimage. 2016;142:394-406. https://doi.org/10.1016/j.neuroimage.2016.08.016
22. Andersson JL, Sotiropoulos SN. An integrated approach to correction for off-resonance effects and subject movement in diffusion MR imaging. Neuroimage. 2016;125:1063-1078. https://doi.org/10.1016/j.neuroimage.2015.10.019

23. Bastiani M, Cottaar M, Fitzgibbon SP, Suri S, Alfaro-Almagro F, Sotiropoulos SN, Jbabdi S, Anderson JLR. Automated quality control for within and between studies diffusion MRI data using a non-parametric framework for movement and distortion correction. Neuroimage. 2019;184:801-812. https://doi.org/10.1016/j.neuroimage.2018.09.073
24. Scherrer B, Schwartzman A, Taquet M, Sahin M, Prabhu SP, Warfield SK. Characterizing brain tissue by assessment of the distribution of anisotropic microstructural environments in diffusion-compartment imaging (DIAMOND). Magn Reson Med. 2016;76(3):963-77. https://doi.org/10.1002/mrm.25912
25. Le Bihan D, Lima M. Diffusion magnetic resonance imaging: what water tells us about biological tissues. PLoS Biol. 2015;13(7):e1002203. https://doi.org/10.1371/journal.pbio.1002203
26. Jeurissen B, Tournier J-D, Dhollander T, Connelly A, Sijbers J. Multi-tissue constrained spherical deconvolution for improved analysis of multi-shell diffusion MRI data. Neuroimage. 2014;103:411-426. https://doi.org/10.1016/j.neuroimage.2014.07.061
27. Tournier JD, Calamante F, Connelly A. Improved probabilistic streamlines tractography by 2nd order integration over fibre orientation distributions. Proceedings of the international society for magnetic resonance in medicine. (Vol. 1670). 2010.
28. Tournier JD, Smith R, Raffelt D, Tabbara R, Dhollander T, Pietsch M, Christiaens D, Jeurissen B, Yeh C-H, Connelly A. MRtrix3: A fast, flexible and open software framework for medical image processing and visualization. Neuroimage. 2019;202:116137. https://doi.org/10.1016/j.neuroimage.2019.116137

29. Avants BB, Epstein CL, Grossman M, Gee JC. Symmetric diffeomorphic image registration with cross-correlation: evaluating automated labeling of elderly and neurodegenerative brain. Med Image Anal. 2008;12(1):26-41. https://doi.org/10.1016/j.media.2007.06.004
30. Delinte N, Dricot L, Macq B, Gosse C, Van Reybroeck M, Rensonnet G. Unraveling multi-fixel microstructure with tractography and angular weighting. Front Neurosci. 2023;17:1199568. https://doi.org/10.3389/fnins.2023.1199568.
31. Fields RD. A new mechanism of nervous system plasticity: activity-dependent myelination. Nat Rev Neurosci. 2015;16(12):756-67. https://doi.org/10.1038/nrn4023